Spectroscopical analysis of wet chemical processes

Martin Zimmer, **Antje Oltersdorf**, **Jochen Rentsch** & **Ralf Preu**, Fraunhofer Institute for Solar Energy Systems (ISE), Freiburg, Germany

This paper first appeared in the third print edition of *Photovoltaics International* journal.

ABSTRACT

Crystalline silicon solar cell fabrication involves many wet chemical process steps. Like most processes in solar cell manufacturing, many of these wet chemical processes were transferred from the semiconductor industry. In contrast to microchip fabrication with maximum throughputs of 100 wafers/hour, state-of-the-art solar cell equipment relies on several 1,000 wafers/hour. Furthermore, specific processes have been developed for the texturisation of the wafer surface. Therefore, there is a need for dedicated methods of characterization of these wet chemical processes. Fraunhofer ISE has developed several analytical methods such as titration, ion chromatography and near infrared (NIR) spectroscopy for the complete analysis of the chemical composition of wet chemical processes baths. These methods were compared considering the inline/online capability, measurement cycle and running costs, with the result that NIR spectroscopy was identified as a complex but very powerful tool for process characterization, as outlined in this paper.

Introduction

Quality control methods gain more and more importance throughout the production chain of crystalline silicon solar cells. For most of the relevant process steps, control measurements of changing wafer or process conditions have to be taken at least in a batch-wise mode, as the process conditions can typically be kept quite stable, with the only changing parameter being the wafer material itself. Control of emitter diffusion processes may serve as an ideal example, where the resulting emitter sheet resistivity typically does not change instantaneously.

For wet chemical processes, this picture is becoming more complex.

In typical etching processes, e.g. for texturisation, it is not only anticipated that the process conditions will change during the course of the process, but that the bath constituents themselves might also change as more and more silicon is dissolved into the bath.

As an example, the dissolution of silicon and formation of hexafluorosilicic acid

(H_2SiF_6) in an acidic etching mixture is shown in the following equation:

$$3Si + 18HF + 4HNO_3 \rightarrow 3H_2SiF_6 + 4NO + 8H_2O$$
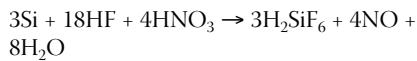
While the silicon removal per wafer, e.g. the etching rate, can be also adjusted in certain process latitudes by variation of the bath temperature, the etching properties depend mainly on the concentrations of HF, HNO_3 and H_2SiF_6 [1].

Additionally, bath constituents such as alcohol are present in alkaline texturing processes, and are in turn lost due to evaporation into the exhaust system as a result of their low vapour pressure. Exact online control and knowledge of the bath constituents are in this case mandatory to stabilize the etch quality.

Another important motivation for exact etching bath control is the determination of the end-of-bath-lifetime, e.g. the determination of the critical bath lifetime after which it is impossible to maintain the etching properties only by redosing with fresh chemicals. Therefore, the exact knowledge of the bath constituents allows the maximum usage of the involved chemistry.

Constant process monitoring in silicon solar cell production features several wet chemical processes of note. For the fabrication of standard screen-printed industrial solar cells, there are a number of relevant wet chemical processes, mainly for texturisation and cleaning purposes. While one-component systems like pure HF for oxide removal are easy to monitor, – i.e. by conductivity measurement, typical texturisation processes are, due to the number of constituents, much more complex.

For acidic texturisation of multi-crystalline silicon wafers, typical mixtures involve amounts of hydrofluoric acid (HF), nitric acid (HNO_3) and water [2]. There have been cases where mixtures featuring additional additives such as phosphoric acid (H_3PO_4) [3], acetic acid (HOAc) [3] and sulphuric acid (H_2SO_4) [4] have been used.

In alkaline random pyramid texturisation for monocrystalline wafers, a base like potassium hydroxide (KOH) or sodium hydroxide (NaOH) and an organic additive like isopropanole (IPA) are used [5].

In addition to these processes, recently developed high efficiency cell concepts require several additional wet chemical process steps like advanced cleaning processes, chemical edge isolation or single-side oxide removal processes. In order to obtain continuously stable and reproducible process results, a reliable monitoring of the bath concentrations is essential.
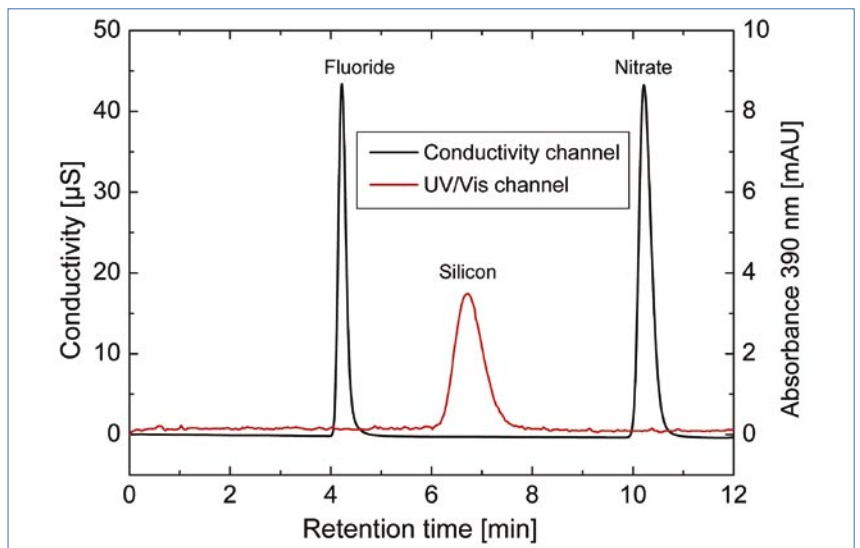

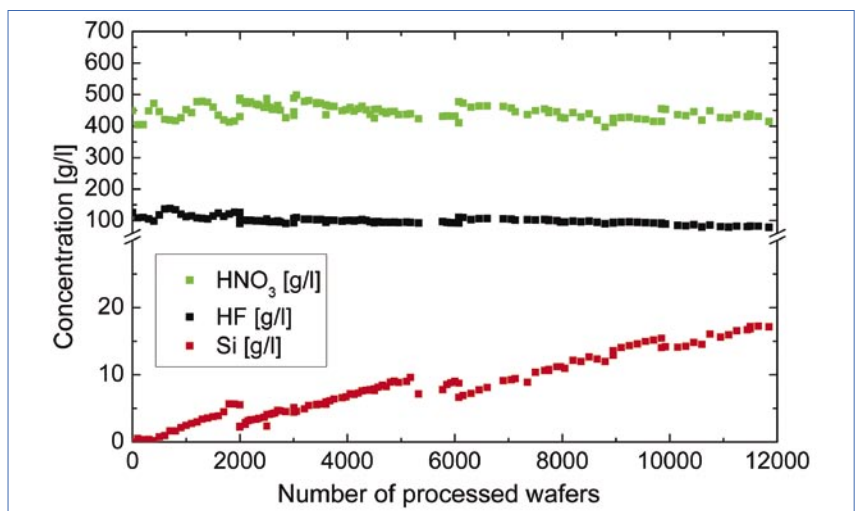**Figure 1. Chromatogram of a mixture of HF, HNO_3 and H_2SiF_6.**

Figure 2. Development of the concentrations of HF, HNO_3 and H_2SiF_6 during the texturisation of 12,000 mc-si wafers.

State-of-the-art analysis techniques

Titration

A very well known and robust method for the determination of ionic species is titration, a versatile method that is suitable for the determination of the main components in almost all wet chemical process baths. For the alkaline texturisation bath, the concentrations of alkaline hydroxide, alkaline silicate and alkaline carbonate can be measured in one single titration.

The concentrations of ammonium hydroxide (NH_4OH) and hydrochloric acid (HCl) in cleaning processes can be detected by pH-titration; the content of hydrogen peroxide (H_2O_2) is measurable by a potentiometric titration with potassium permanganate ($KMnO_4$).

In acidic texturisation baths hydrofluoric acid (HF), nitric acid (HNO_3) and the reaction product hexafluorosilicic acid (H_2SiF_6) are accessible via titration [6,7]. Due to the similarity of the pKa-values of the four acids – H_2SiF_6 is a divalent acid – the determination of the three concentrations has to take place in two steps. In the first pH titration, the total acid amount and the concentration of hexafluorosilicic acid are measured. The second step is a potentiometric titration, where lanthane nitrate ($La(NO_3)_3$) is used to precipitate the fluoride ions. The decreasing fluoride concentration is monitored with a fluoride ion sensitive electrode (F-ISE), while the total consumption of the present fluoride ions appears as an inflection point in a graph, where the potential of the F-ISE is plotted against the volume of $La(NO_3)_3$. The concentrations of HF, HNO_3 and H_2SiF_6 can be calculated from the total acid amount, the concentration of dissolved silicon and the total fluoride concentration from the second titration.

	J_{sc} [mA/cm²]	V_{oc} [mV]	FF [%]	η [%]
Average	31.6	604	76.9	14.7
Relative Standard Deviation	0.3%	0.9%	0.6%	1.5%

Table 1. Solar cell results for 100 neighbouring mc-Si solar cells.

Ion chromatography

Another method for the determination of main components is liquid chromatography. In this process, the sample is injected in a liquid mobile phase, which is pumped through the chromatographic column, where the species are separated. A detector on the column outlet detects the arriving particles; the signal intensity is proportional to the component's concentration.

Organic additives like isopropanol can be separated in a high performance liquid chromatography (HPLC)-System and measured in a refractive index detector. The anions and cations of acids and bases are separated in ion exchange columns and quantified via electrical conductivity measurement.

The measurement of the silicate concentration is more difficult, particularly with regard to acidic texturisation baths, since silicic acid is a very weak acid and shows nearly no intrinsic conductivity. One possibility is the precipitation of H_2SiF_6 with potassium chloride in cold ethanol [8]. The precipitate is then dissolved and hydrolyzed in a sodium hydroxide solution. The hexafluorosilicate concentration is then measured indirectly via the fluoride amount. The precipitation is a very time-consuming and labour-intensive procedure and as a result is not a suitable technique for use in routine analysis.
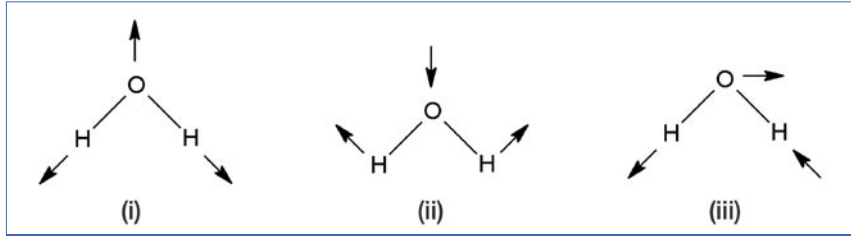

Figure 3. Normal vibration modes of the H_2O-molecule.

A more practicable approach is the postcolumn derivatisation of silicon [9]. After passing the electrical conductivity measurement cell, a derivatisation reagent is added to the eluent flow. The silicic acid reacts with sodium molybdate; the resulting molybdosilicic acid is a yellow complex, which can be detected in a UV/Vis-detector at 390nm.

Figure 1 shows a chromatogram of an acidic texturisation solution, recorded with postcolumn derivatisation. The black graph shows the conductivity channel while the red graph shows the absorption at 390nm after the derivatisation reaction. Fluoride ions from the hydrofluoric acid and nitrate ions from the nitric acid appear as peaks in the conductivity channel at retention times of 4.1 minutes and 10.1 minutes, respectively. The silicon peak arises at 6.6 minutes in the UV/Vis channel.

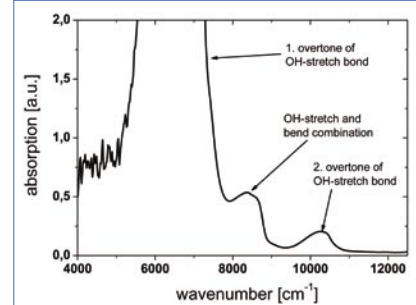The capability of this system was tested in the photovoltaic technology evaluation

Figure 4. Near-infrared spectrum of pure water.

center (PV-TEC) at Fraunhofer ISE during the texturisation of 10,000 multicrystalline silicon wafers. This texturisation process took place in an inline saw damage etching tool with a bath volume of 170 litres. During the texturisation process, labelled and neighbouring mc-Si wafers (format: 156 x 156mm²; thickness: 240μm; resistivity ρ = 0.5 – 2.0 Ωcm) were etched after each 120
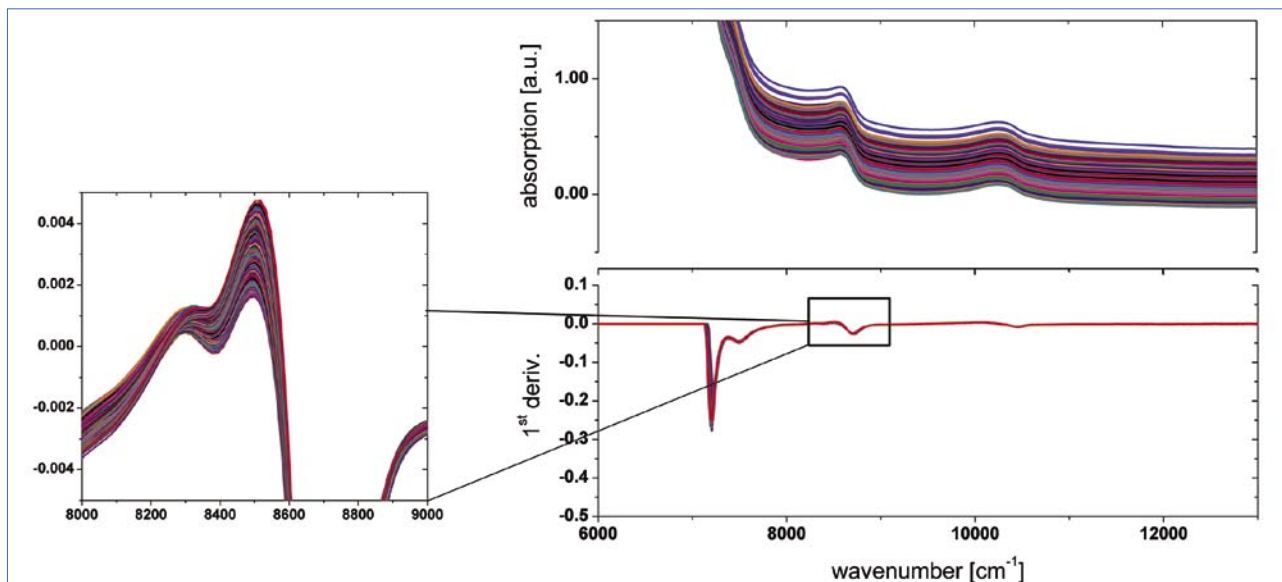
Figure 5. Calibration dataset of 661 near infrared spectra with different concentrations of HF, HNO₃ and H₂SiF₆. The baseline shift in the original spectra is eliminated by calculating the first deviation. The chemical information remains in slight differences in the peak regions of the spectra.

wafers. A sample of the etching solution was taken for each labelled wafer. Figure 2 shows the concentration plot for the main components in the etching bath. The HF- and HNO₃-concentration were kept constant, while the silicon concentration increased. The labelled wafers were processed as solar cells (the main parameters of the illuminated current-voltage measurement are shown in Table 1). The low relative standard deviation of the cell parameters is an indicator of a stable texturisation process.

NIR spectroscopy: a real inline measurement technique

Principles of NIR spectroscopy

A widely used method for the process control in pharmaceutical and chemical industries is NIR spectroscopy [10]. This measurement principle is based on the observation of vibrational-spectral transitions between energy levels that differ by two or more vibrational quantum number units. According to the quantum mechanical model of the harmonic oscillator, these transitions are not allowed, but, due to the anharmonicity of real molecular oscillator systems, overtone and combination bands are observed in the wave number range between 4,000 and 12,500cm⁻¹.
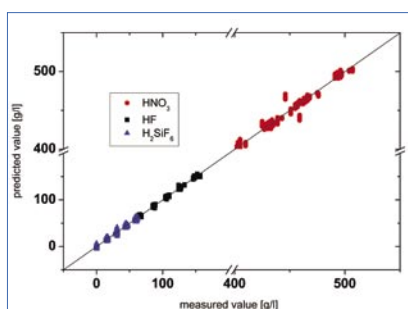

Figure 6. Calibration curve for H₂SiF₆, HF and HNO₃.

One such oscillation system is the water molecule, which contains two OH bindings so that three different vibration modes are possible. The first mode is a symmetric stretch vibration (Figure 3(i)), the second is the bending mode (Figure 3(ii)), and the third is the asymmetric stretch mode (Figure 3(iii)) [11].

Figure 4 shows an NIR spectrum of pure water at 20°C with a path length of 0.375 inches. Three bands are visible: the first overtone of the OH stretch bond at 6,500cm⁻¹ (which cannot be completely resolved at the given conditions); the OH stretch and bend combination at 8.300cm⁻¹ and the second overtone of the OH-stretch bond at 11,000cm⁻¹.

It is known that many inorganic components like hydrofluoric acid (HF) or potassium hydroxide (KOH) do not show any infrared active vibrations. As these components are completely dissociated in aqueous solutions, the resulting (respective) fluoride ion and potassium ion are monoatomic ions where vibrations are not possible. Others like the nitrite ion have vibrations with very low excitation energies, thus the bands do not occur in the observed NIR-region.

However, even if there are no directly observable absorption bands in the NIR-spectra, the presence of inorganic ionic components affect the appearance of the spectra of water. This is due to the perturbation of the well-regulated molecular water structure. This perturbation leads to small shifts in vibration anharmonicity and energy levels and therefore to shifts in the peaks' height and location.

This leads to the insight that simple calibration methods like the use of 'Beer's law,' where the absorption at a certain wavelength is proportional to the chemical concentration, must fail when used in these circumstances. Even multivariate calibration approaches like the 'classical least squares' algorithm is not usable, since the mathematical precondition for the usage of this calibration is an exact knowledge and quantification of all parameters that influence the spectra. This can be avoided by using such nonlinear calibration algorithms as the principal component regression (PCR) or the partial least squares (PLS) algorithm [12].

NIR spectroscopy in acidic texturisation

The calibration model for acidic texturisation contains a model for hydrofluoric acid, nitric acid and hexafluorosilicic acid. None of these three species show separate vibration bands in the near infrared region, and so require a nonlinear algorithm. In contrast to titration, where only the titer of the stock solutions has to be determined, or ion chromatography, where each component can be calibrated separately, the interaction between the components must not be neglected. Therefore, the calibration samples for one component have not only to cover the calibration range of the examined component, but also the estimated range of all matrix components. This is given by a fractional factorial design, where five concentrations are realized for each of the three components. The resulting experimental design contains 62 calibration samples, which were prepared from pure acids. Hydrofluoric acid was calibrated in the 70 – 120g/l range; nitric acid was calibrated between 380 – 520g/l and dissolved silicon in the range from 0 to 60g/l H₂SiF₆.

Adjacent to the presence of inorganic species, the temperature has a high influence on the appearance of the NIR-spectra. To compensate for the temperature's effect, each calibration sample was measured at temperatures between 5°C and 15°C. All spectra were measured with a FTPA 2000 FT-NIR spectrometer (ABB, Québec, Canada).

After the elimination of outliers, the calibration dataset consisted of 661 spectra with exact knowledge of the HF-, HNO$_3$- and H$_2$SiF$_6$-concentrations (see Figure 5). In the peak-free region near 12,000cm^{-1}, where no chemical information is expected, a baseline shift is observed. This shift can be eliminated by calculating the first derivation of the absorbance spectra. The chemical information remains in slight differences in the peaks of the first derivation.

The calculated models for HF, HNO$_3$ and H$_2$SiF$_6$ are validated via cross validation. For each sample, a model is calculated, leaving out the actual sample. The predicted concentration is then compared with the given concentration of the sample. The Standard Error of Validation (SEV) can then be calculated from the square sum of these residuals. It gives a first impression of the quality of the calibration model. A more detailed overview of the methodical approach is given in [12]. In Figure 6, the predicted concentrations from the cross validation are plotted against the given concentrations. A good compliance is observed for all three components.

The cross validation is only a first order quality parameter. During real texturisation processes, other parameters like gas bubbles or nitrogen oxides can influence the prediction quality of the NIR model. Therefore, a validation experiment was executed where the evidence of the PLS-models was tested. In this experiment, a solution of HF and HNO$_3$ was prepared

Titration	Ion Chromatography	NIR spectroscopy
✓ Easy and robust	✓ Very flexible	✓ Very fast method
✓ Low cost method	✓ No preparation Stepps	✓ Real inline-method
	✓ Easy calibration	✓ No maintenance
✗ Not extensible	✗ High maintenance	✗ Very time-consuming calibration
✗ Slow method	✗ Indirect determination of HF	
✗ Sample preparation		
✗ Indirect determination of HF and HNO$_3$		

Table 2. Comparison of the different analysis techiques.

from pure acids. Nine carriers with five small wafer pieces (30x30mm^2) were etched in 250ml of the etching solution. The concentrations in the solution were measured continuously by NIR spectroscopy, and validation measurements were carried out with ion chromatography and titration.

Figure 7 shows the concentration plots for HF, HNO$_3$ and H$_2$SiF$_6$ during the texturisation process. In the first period the solution was cooled down from 22°C to 9°C. During this cooling-down phase, no concentration shifts are visible, suggesting that the NIR models are not temperature dependent. The etching process shows an increasing silicon concentration and decreasing HF- and HNO$_3$- concentrations due to the consumption of HF and HNO$_3$ in the reaction with silicon. Under the given etching conditions, nitrogen oxide bubbles occur, which are responsible for the higher noise and the observed spikes in the concentration graphs.

To investigate the precision of the developed NIR model, samples were taken during the etching process and then measured with titration and ion chromatography. To compare the offline-measured results with these from the inline NIR measurement, the concentrations are plotted as dots in Figure 7. In the limits of the reached accuracy of the used methods, no differences are found between titration, ion chromatography and NIR spectroscopy.

Conclusion

To date, three different methods are available for the chemical analysis of wet chemical process baths in solar cell fabrication. These methods differ in many aspects, regarding inline capability, running cost, flexibility and calibration workload. An overview is given in Table 2.

Titration is a very robust and widely used method for the determination not only of acids and bases, but also the concentrations

[8] Acker, J. & Henßge, A. 2007, *Talanta*, 72, p. 1540.

[9] Zimmer, M. et al 2007, *Proceedings of the 22nd European Photovoltaic Solar Energy Conference.*

[10] Siesler, H. W. 1995, *NIR News* 6(1).

[11] Siesler, H. W. 2002, 'Near-Infrared Spectroscopy,' Wiley-VCH Weinheim.

[12] Sharaf, M. A., Illman, D. L. & Kowalski, B. R. 1986, 'Chemometrics,' Wiley New York.

About the Authors

Martin Zimmer graduated in 2005 with a diploma in chemistry from the Ruprecht-Karls-University in Heidelberg, specializing in spectroscopical methods for microbiological applications. He joined Fraunhofer ISE in 2006 and is currently pursuing a Ph.D. in the field of wet chemical analysis and process development within the group for Wet Chemical and Plasma Technologies at ISE.

Antje Oltersdorf studied process engineering at TU Hamburg-Harburg. During her diploma thesis at Fraunhofer ISE, she investigated ion chromatographic and titration methods for acidic texturizations. Since 2008, she has been working on her Ph.D. thesis on trace element analytics in wet chemical processes.

Jochen Rentsch is Head of the Wet Chemical and Plasma Technologies/ Process Transfer group at Fraunhofer ISE. He received his degree in physics in 2002 from the Albert-Ludwigs University of Freiburg, Germany. His Ph.D. research at Fraunhofer ISE was in the field of plasma etching technologies and their application to industrial solar cell processing.

Ralf Preu is Head of the Department for PV Production Technology and Quality Assurance at Fraunhofer ISE. He received a diploma degree in physics in 1996 from the University of Freiburg, Germany, a Ph.D. degree in electrical engineering in 2000 and a diploma degree in economics in 2003 from the University of Hagen.
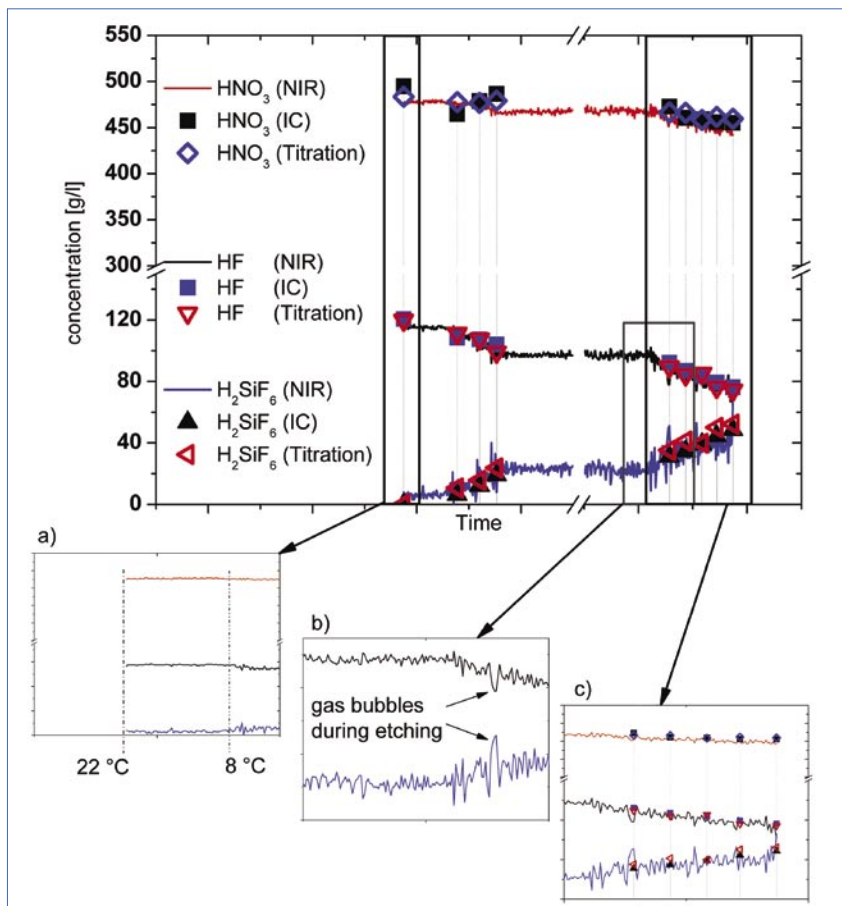
Figure 7. Concentrations of HF, HNO₃ and H₂SiF₆ during the validation experiment. The temperature independency is shown in (a) where the calculated concentrations remain constant during the cooling-down phase. (b) shows the influence of gas bubbles in terms of spikes in the concentration course. Good compliance of concentration between measurements taken with titration and ion chromatography are shown in (c).

of oxidizing agents like hydrogen peroxide. Maintenance and calibration costs are quite low, since most of the used stock solutions are commercially available. The measurement cycle is in the range of 10 to 15 minutes. A constraint for the usage of the titration is the limited number of components that can be detected simultaneously. Acidic texturisation is an example where additional titration steps become necessary for the analysis of all components. The determination of organic components like isopropanol is not possible.

A faster and more flexible method is chromatography, which process allows measurement of inorganic acids and bases and organic additives in cycles that are usuallly shorter than 10 minutes. Commercially available high-end equipment has a high automation level that can reduce the running costs to a minimum. Despite the high automation level, a sample preparation step and hence a contact with corrosive media is necessary for both titration and chromatography. A real inline system can be realised with NIR spectroscopy.

Since NIR spectroscopy is a nonselective method, interactions between the measured components as well as the influence of varying temperatures have to be included in the calibration dataset. This can lead to a high workload, which can be offset by the fact that calibration models for most purposes in photovoltaic industries are commercially available. After setting up a calibration model, further maintenance requirements are minimal. Modern FT-NIR instruments reach a measurement cycle of 30 seconds so that NIR spectroscopy enables a real-time process control.

References

[1] Schwartz, B. & Robbins, H. 1976, *Journal of The Electrochemical Society*, 123, p. 1903.

[2] Einhaus, R. & Vazsoniy, E. 1997, *Proceedings of the 26th IEEE Photovoltaic Specialists Conference.*

[3] Nishimoto, Y., Ishihara, T. & Namba, K. 1999, *Journal of The Electrochemical Society*, 146, p. 457.

[4] Park, S. W., Kim, J. & Lee, S. H. 2003, *Journal of the Korean Physical Society*, 43, p. 423.

[5] Vazsonyi, E. et al 1999, *Solar Energy Materials & Solar Cells*, 57, p. 179.

[6] Henßge, A., Acker, J. & Müller, C. 2006, *Talanta*, 68, p. 581.

[7] Henßge, A. & Acker, J. 2007, *Talanta*, 73, p. 220.